

## Surface-wave analysis for estimating near-surface properties

Khaled Al Dulaijan and Robert R. Stewart

### ABSTRACT

In a real layered earth, surface waves are dispersive with multiple modes. The dispersion properties of surface waves can be useful for estimating  $S$ -wave velocity of the near surface. The surface-wave analysis, in the Priddis site, involves recording of surface waves on vertical geophones, estimating phase-velocity dispersion curves, and then inverting these dispersion curves to estimate the  $S$ -wave velocity, of the near surface, as a function of depth.  $P$ -wave velocities of the near surface were estimated from the sonic log of the Priddis well, and samples from the well cuttings were described in the lab for lithology information of the near surface.

### INTRODUCTION

In seismic surveys, usually more than two third of seismic energy is imparted into Rayleigh waves when a  $P$ -wave source is used (Park et al., 1999). These waves are non-dispersive in the case of propagation along the surface of an isotropic homogeneous halfspace, but they are dispersive with multiple modes in a real layered earth. Dispersion properties of surface waves can be useful for estimating  $S$ -wave velocity. The dispersion of surface waves has been studied by many authors (i.e. Rayleigh, 1887; Sezwa, 1927; Thompson, 1950; Dobrin, 1951; and Haskell, 1953). Surface-wave methods were developed for geotechnical engineering and  $S$ -wave reflection seismology purposes to estimate  $S$ -wave velocity of near-surface materials. Implementation of such techniques involves recording Rayleigh waves on vertical-component geophones, estimating phase-velocity dispersion curves for Rayleigh waves, and then inverting these dispersion curves to estimate  $S$ -wave velocity as a function of depth.

Current inversion techniques for surface-wave methods assume a horizontally layered earth model consisting of homogeneous and isotropic layers. These techniques are different in the computation of the forward model and the method of optimization. Derived  $S$ -wave velocity information can be useful in foundation dynamics, pavement analysis, soil improvement, static correction of  $S$ -wave reflection data (Pelton, 2005).

The process workflow for our surface wave analysis study in Priddis is outlined in Figure 1. The data was processed using *SurfSeis 2.05*, software created by Kansas Geological Survey. The purpose of our study is to obtain  $S$ -wave velocity for the near surface.

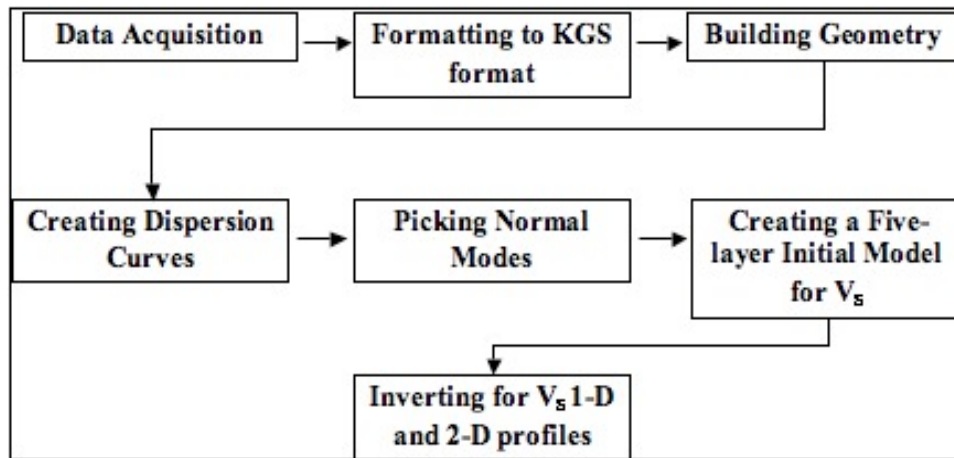


FIG. 1. Process workflow for surface wave analysis in Priddis.

## STUDY AREA

The study area is located at the Rothney Astrophysical Observatory site, 25 km southwest of Calgary. The study area is indicated by the red circle, shown on the surface geology map in Figure 2. The two-dimensional seismic line, which was acquired as an activity of 2007 University of Calgary field school, is shown in Figure 2. Shallow well was drilled, and is indicated by the red dot on Figure 2 as well. Figure 3 shows a photograph of Priddis site with the well indicated by the red “A”. Figure 4 shows the elevation profile along the line. The line is 403 m long from southeast to northwest. The elevation is high (1268) in the southeastern part of the line, and lower (1252 meters) in the northern part of the line. The data processed is the 180 meters of the northwestern part of the line.

The surface geology, of the study area, consists of the Paskapoo formation. The Paskapoo formation, which is dominated by shale and sandstone, is the largest groundwater source in the Canadian Prairies. The samples of well cuttings were described in the lab. Table 1 shows the description of the samples, and Figure 5 shows the lithology log of the near surface. The near surface consists of the Paskapoo clastics. *P*-wave velocities of the near surface were calculated from the sonic log of the well, and shown in Table 2. The upper 3.9 m shows extremely low *P*-wave velocity, about 600 m/s. This overburden layer consists of sandstone and clay particles. The lower layers are more compacted clastics, and have higher *P*-wave velocities.

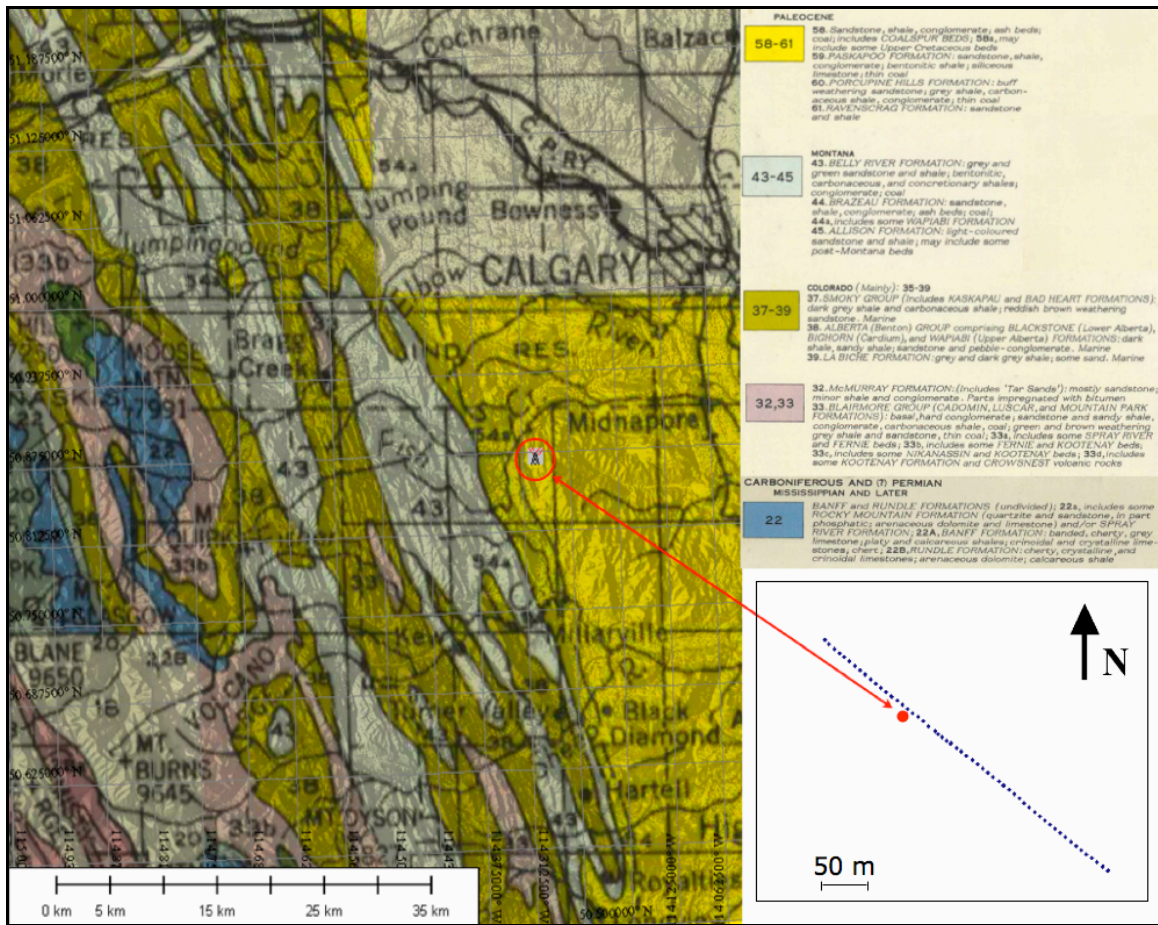


FIG. 2. Location map showing: surface geology, well, and two-dimensional refraction seismic line.



FIG. 3. Priddis site.

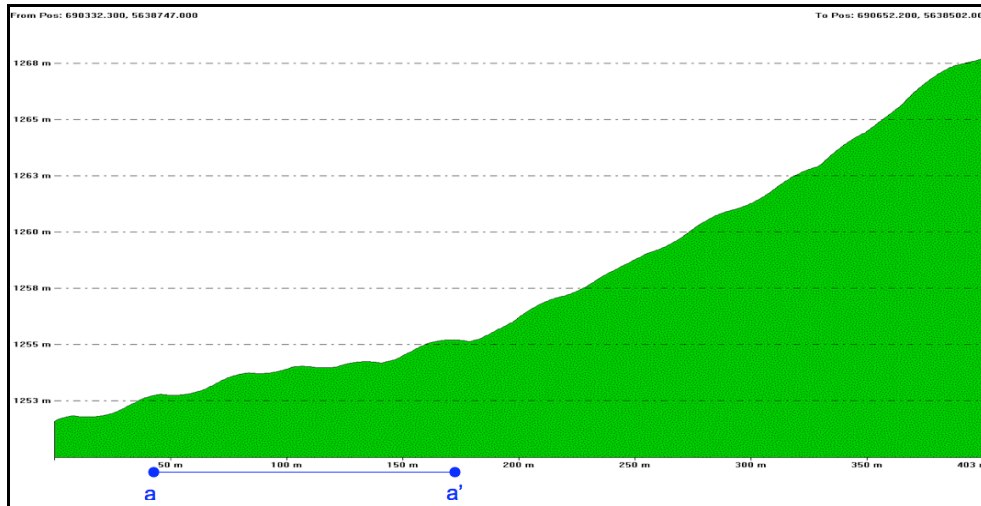


FIG. 4. Elevation profile.

Table 1. Samples (from well cuttings) descriptions.

Depth (m)	Sample Description
0-2.1	<b>50% Sandstone:</b> Transparent, translucent in part, very fine to medium, sub-angular to sub-rounded, moderately sorted, loose, and low porosity. <b>50% Clay:</b> Tan to brown, friable, and calcareous.
2.1-4.0	<b>70% Sandstone:</b> Transparent, translucent in part, fine to medium, sub-angular to sub-rounded, moderately to well sorted, loose, and low porosity. <b>30% Clay:</b> Tan to brown, soft, and calcareous.
4.0-18.0	<b>100% Sandstone:</b> Mainly translucent, transparent and white in part, very fine to coarse, angular to sub-rounded, moderately sorted, moderately compacted, and low porosity.
18.0-22.0	<b>100% Shale:</b> Gray, blocky, sub-fissile in part, moderately indurated, and highly calcareous.
22-23.2	<b>80% Sandstone:</b> Transparent, tan, very fine to medium, angular, moderately sorted, well compacted with calcareous cement in part, and low porosity. <b>20% Shale:</b> Gray, blocky to sub-blocky, and well-indurated.
23.2-23.8	<b>100% Shale:</b> Gray, blocky, well indurated, and calcareous.
23.8-28.3	<b>100 % Siltstone:</b> light gray, tan in part, blocky, moderately indurated, slightly calcareous.
28.3-31.1	<b>100 % Siltstone:</b> light gray, tan in part, blocky, moderately to well indurated, calcareous.

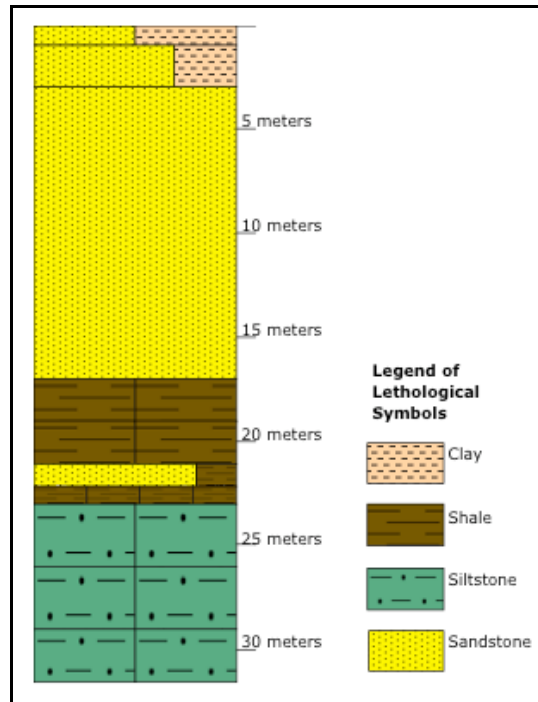


FIG. 5. Lithology log from the Priddis well.

Table 2. *P*-wave velocity (from sonic log).

Depth (m)	<i>P</i> -wave velocity (m/s)
0-3.9	1600
3.9-17.6	1900
17.6-28.3	2080
28.3-39.3	2250

### DATA ACQUISITION

The 2-D seismic line was acquired by the students of the field school 2007 class. The source used for this two-dimensional seismic line is a five-pound sledgehammer. Ten Hz vertical geophones were used as receivers. A fixed array was used with 180 m spread length, and 72 receivers. Receiver spacing is 2.5 m, and source spacing is 12.5 m. The near offset is ranges between 0 and 37.5 m. Illustration of the field outlay is shown in Figure 6. The record length is 600 ms with 0.125 ms sampling rate. The record length is short, and that will negatively affect the accuracy of the inverted *S*-wave velocity profile of the near surface. Figure 7 shows a shot gather, located within 2.5 m from the well. Most of the energy on this shot gather is surface wave with no significant body wave present.

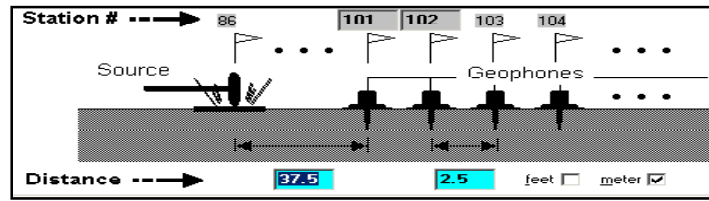


FIG. 6. Field acquisition layout.

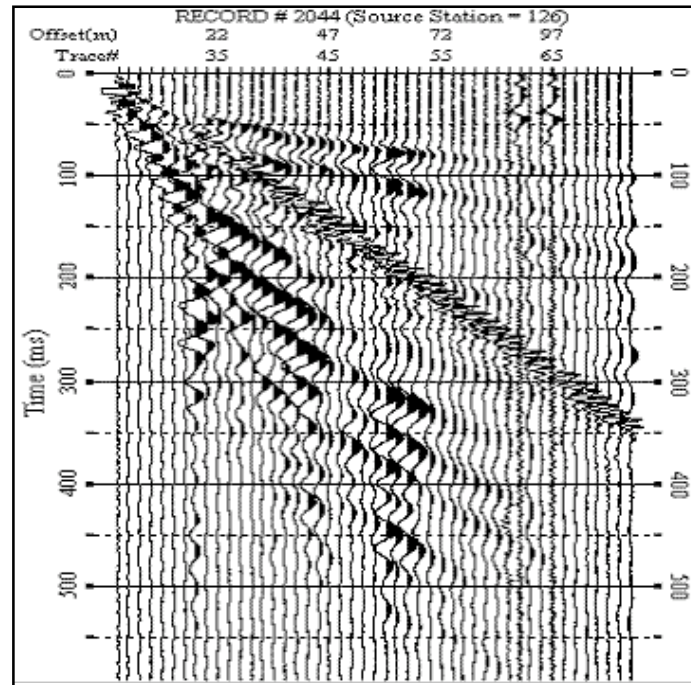


FIG. 7. Shot gather.

### Velocity Dispersion of Rayleigh Waves

In the case of homogeneous half space, the Rayleigh wave is not dispersive, and has a velocity equal to the  $S$ -wave velocity multiplied by 0.9491 if the Poisson's ratio is 0.25. On the other hand, Rayleigh wave is dispersive for a layered earth. Lower frequencies penetrate deeper, have greater phase velocity, and are more sensitive to deeper layers. Higher frequencies have less phase velocity and are more sensitive to the physical properties of the near-surface layers.

The phase velocity of surface wave of a layered earth model is a function of frequency and four earth parameters, which are  $P$ -wave velocity ( $V_P$ ),  $S$ -wave velocity ( $V_S$ ), density ( $\rho$ ), and the thickness ( $h$ ) (Xia et al., 1999). The Rayleigh wave propagates in several discrete modes. The phase velocity,  $c$ , and the group velocity,  $v$ , of each mode depends on frequency. The phase velocity and the group velocity are related as follows

$$c = v \left[ 1 - \frac{f}{c} \frac{dc}{df} \right], \quad (1)$$

where  $f$  is the frequency. If no dispersion is present, then the phase and the group velocities are equal. If the phase velocity is decreasing when the frequency increases, then the phase velocity is greater than the group velocity, and that is called normal dispersion (Al-Husseini et al., 1981)

### DISPERSION CURVES

The dispersive surface wave on the shot gather, shown in Figure 7, has a velocity ranging from 270 m/s to 890 m/s, as illustrated in Figure 8. A dispersion curve, for this shot, was created using *SeisSurf 2.05*, as shown in Figure 9. This software uses a transformation method different than the slowness-frequency ( $p-\omega$ ) method of McMechan and Yedlin (1981). When using the slowness-frequency ( $p-\omega$ ) method, the dispersion curve is created by two linear transformations: a slant stack of the data to produce a wavefield in the slowness-time intercept ( $p-\tau$ ) plane, and one-dimensional Fourier transform of the ( $p-\tau$ ) wavefield to slowness-frequency ( $p-\omega$ ) domain (McMechan et al., 1981).

A shot gather in space-time domain,  $u(x,t)$ , is transformed to the space-angular frequency domain,  $U(x,\omega)$ , using forward Fourier Transform as follows

$$U(x,\omega) = \int u(x,t)e^{i\omega t} dt, \quad (2)$$

where  $\omega$  is the angular frequency.  $U(x,\omega)$  can be represented as the multiplication of the phase spectrum,  $P(x,\omega)$ , and the amplitude spectrum,  $A(x,\omega)$

$$U(x,\omega) = A(x,\omega)P(x,\omega). \quad (3)$$

The phase spectrum contains the dispersion information, and the amplitude spectrum contains all other information, such as attenuation.  $U(x,\omega)$  can be express as follows:

$$U(x,\omega) = A(x,\omega)e^{-i\phi x}, \quad (4)$$

where  $\phi = \frac{\omega}{c_\omega}$ , and  $c_\omega$  is the phase velocity. Now, we apply a transformation, that can be thought of as summing over the offset of wavefield of a frequency after applying offset-dependent phase shift,  $\theta$ , as follows

$$V(\omega, \theta) = \int e^{i\theta x} [U(x, \omega) / |U(x, \omega)|] dx = \int e^{-i(\phi - \theta)x} [A(x, \omega) / |A(x, \omega)|] dx. \quad (5)$$

This will have a maximum at  $\phi = \theta = \frac{\omega}{c_\omega}$ .  $c_\omega$  can be estimated where peak of  $V$  occurs.

For a given value  $\omega$  in the wavefield  $I(\omega, c_\omega)$ , the peaks along the  $c_\omega$  axis will determine the dispersion curve (Park et al., 1998).

From the well data, we estimate the  $S$ -wave velocity to be around 200 m/s. The cutoff frequency,  $f_{cn}$ , of the  $n^{\text{th}}$  mode is given by

$$f_{cn} = \frac{V_s(n + \frac{1}{2})}{2h}, \quad (6)$$

where  $h$  is the thickness of the layer (Krebes, 1989). Then, substituting 200 m/s for the  $S$ -wave velocity, 4 m for the thickness, and 0 for the mode in Equation (6), will give 12.5 Hz for the cutoff frequency. Therefore, frequencies below 12.5 Hz will not propagate through the first layer. The dispersion curve, shown in Figure 9, has two strong amplitude trends. The one to the left has frequencies below 12.5 Hz, so the other strong trend has been picked as the normal mode, but what about if the normal mode was the other trend? That will not affect much the result, because the picked fundamental mode is used only for the obtaining the initial model, and the inversion is based on examining multiple modes of dispersion.

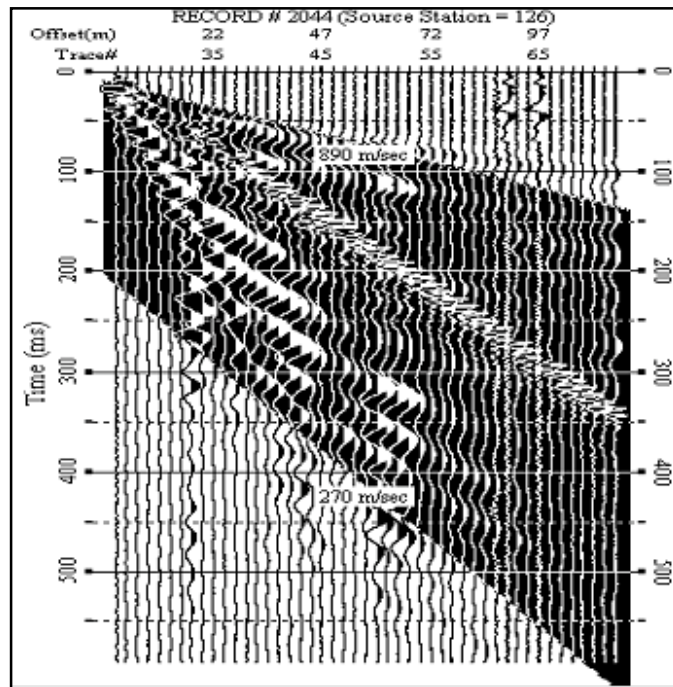


FIG. 8. Shot gather with surface wave (with velocities between 270 and 890 m/s) highlighted.

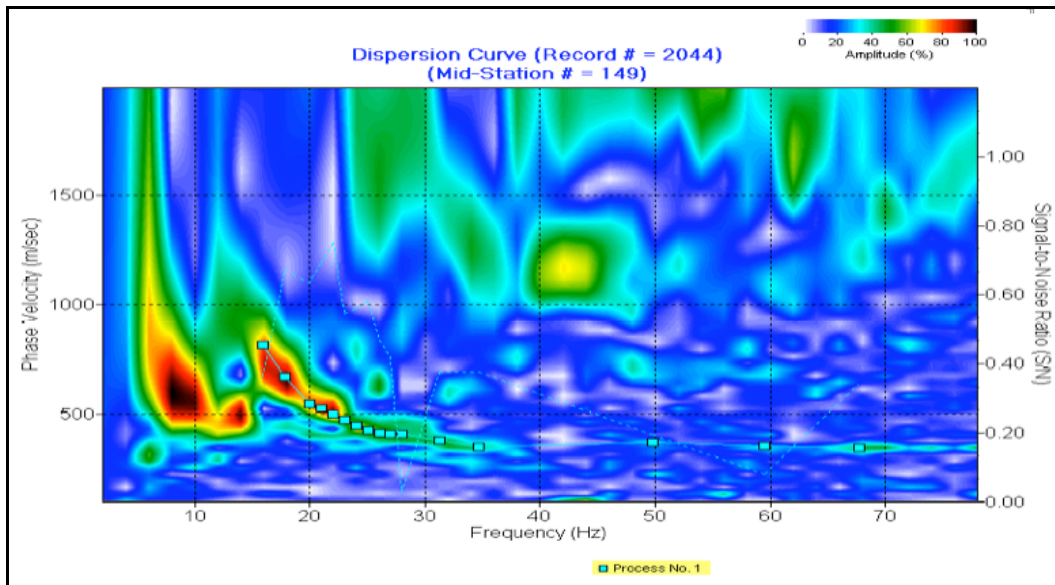


FIG. 9. Dispersion curve.

### INVERSION OF DISPERSION IMAGE

The  $P$ -wave velocities are calculated from the sonic log for five layers. Five-layer  $S$ -wave velocity model was then created by using a constant a Poisson's ratio, equal to 0.405, to construct our initial model of  $S$ -wave velocity that is shown in Table 3. This five-layer model is used as the initial model for the inversion. A better initial model would be one using variable Poisson's ratio based on lithology information.

The *SurfSeis 2.05* is used for inversion. This software applies a general Monte-Carlo method to the dispersion image, rather than the dispersion curve, enabling up to 4 modes to be accounted for. Figure 10 shows the initial model, indicated by the dashed blue line, against the inversion results for  $S$ -wave velocities, indicated by the solid blue line. In general, the inversion results are greater than the initial values. That means the true Poisson's ratios are less than the assumed one, 0.405.

Figure 11 shows a two-dimensional  $S$ -wave velocity profile across the line.  $S$ -wave velocities ranges from 200 m/s to 1400 m/s, and is increasing with depth in general. This  $S$ -wave velocity profile can be related to the (a-a') segment of the elevation profile shown in Figure 4. The lithology log is positioned on the well location of the  $S$ -wave velocity profile, shown in Figure 11. The lithology log correlates well to the  $S$ -wave velocity profile.

Table 3. Initial model.

Layer	Bottom	Thickness	S-Vel (Vs)	P-Vel (Vp)	POS Ratio
1	3.900	3.900	240	600	0.405
2	17.600	13.700	760	1900	0.405
3	28.300	10.700	832	2080	0.405
4	39.300	11.000	900	2250	0.405
5	Half Space	Infinity	980	2450	0.405

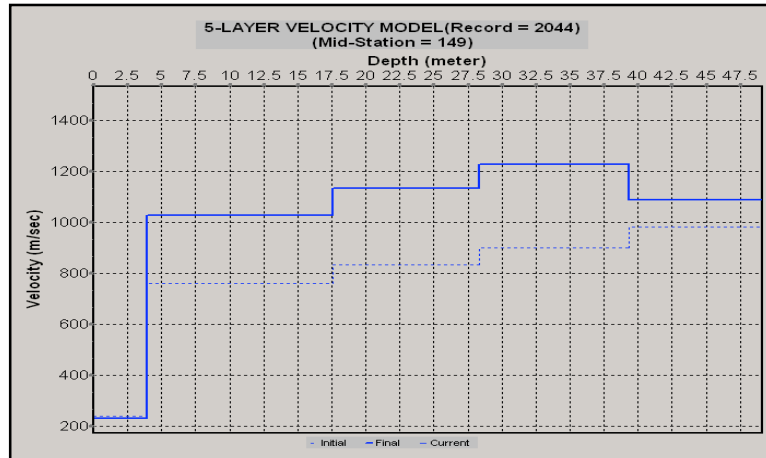


FIG. 10. Inverted S-wave velocity vs. Initial model.

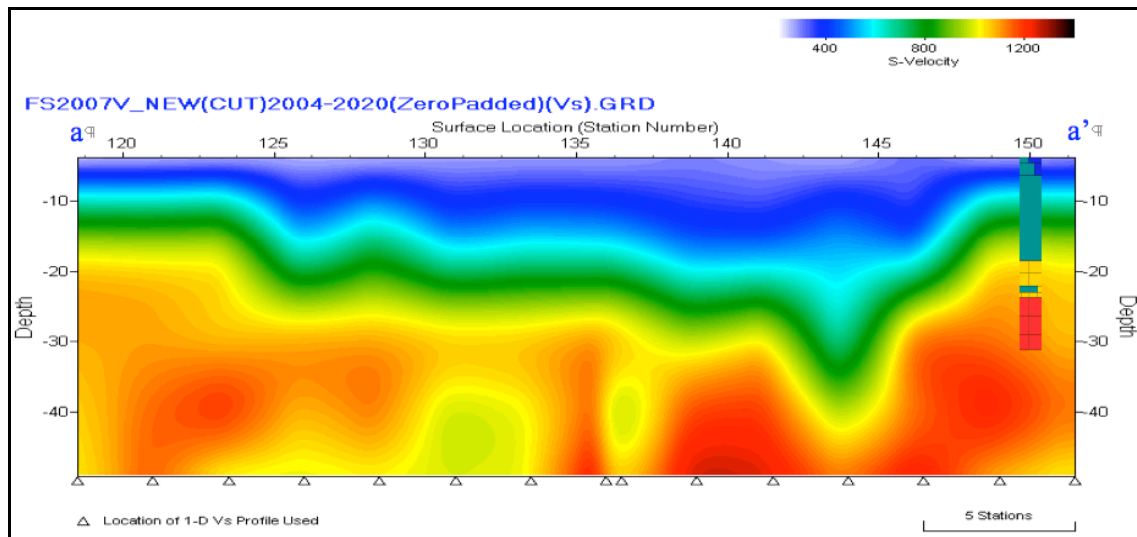


FIG. 11. S-wave velocity two-dimensional profile.

### CONCLUSION

In a real layered earth, surface wave is dispersive with multiple modes. The dispersion properties of surface waves are useful in estimating *S*-wave velocity of the near-surface layers. In Priddis site, surface waves were recorded on vertical geophones, phase-velocity

dispersion curves were created, and then these dispersion curves were inverted to estimate the *S*-wave velocity of the near surface. Our near surface study in Priddis includes analyzing well data. *P*-wave velocity of the near surface was estimated from the sonic log of the Priddis well, and samples from the well cuttings were described in the lab for lithology information of the near surface. The inverted *S*-wave velocity profile shows a good correlation with the lithology log.

### FUTURE WORK

Future work will include:

- Re-acquiring the seismic data with longer record length, and with a three-component land streamer.
- Calculating *S*-wave static corrections using surface-wave methods.
- Calculating conventional *S*-wave static corrections.
- Comparing static corrections, calculated using different methods.

### ACKNOWLEDGMENTS

We would like to thank Kevin Hall, Joe Wang, Henry Bland, and the students of 2007 field school (GOPH-549) for helping in acquiring the data. Also, we thank Timothy Keho, Thierry-Laurent Tonellot, and Christopher Liner from Saudi Aramco, and the Kansas Geological Survey for the use of *SurfSeis 2.05* software. The support of CREWES industrial sponsors is greatly acknowledged.

### REFERENCES

- Al-Husseini, M.I., J.B. Glover, and B.J. Barley, 1981, Dispersion patterns of the ground roll in eastern Saudi Arabia, *Geophysics*, **46**, 121-137.
- Dobrin, M. B., 1951, Dispersion in seismic surface waves, *Geophysics*, **16**, 63-80.
- Haskell, N. A., 1953. The dispersion of surface waves on multilayered media: *Bull. Seis Soc. Am.*, **43**, 17-34.
- Krebes, E., 1989, *Seismic Theory and Methods: Geophysics 551 course notes*, University of Calgary, 4.1-4.18.
- McMechan, G. A., and Yedlin, M. J., 1981, Analysis of dispersive waves by wave field transformation: *Geophysics*, **46**, 869–874.
- Park, C. B., R. D. Millar, and J. Xia, 1998, Imagin dispersion curves of surface waves, Presented at the 68th Ann. Mtg of SEG, New Orleans, Expanded Abstract, 1377-1380.
- Park, C. B., R. D. Millar, and J. Xia, 1999, Multichannel analysis of surface waves: *Geophysics*, **64**, 800-808.
- Pelton, J.R., 2005. Near-Surface Seismology—Surface-Based Methods: *Soc. Explor. Geophys., Investigations in Geophysics No. 13*, Dwain K. Butler, ed., Near-surface Geophysics, 242-247.

Rayleigh, L., 1887, On waves propagated along the plane surface of an elastic solid: Proc. London Math. Soc., **17**, 4-11.

Sezawa K., 1927, Dispersion of elastic waves propagated on the surface of stratified bodies and on curved surfaces. Bull. of the Earthquake-Inst. Imperial Univ. Tokyo, **3**, 1-18

Thomson, W. T., 1950, Transmission of elastic waves through a stratified solid medium, J. Appl. Phys., **21**, 89-93.

Xia, J., Miller, R. D., and Park, C. B., 1999, Estimation of near-surface shear-wave velocity by inversion of Rayleigh wave: Geophysics, **64**, 691–700, this issue.